

The TESS Atlas: an open source catalog of TESS transit fits

AUTHOR LIST TBD

ABSTRACT

We present the first TESS Atlas, a transiting exoplanet parameter estimate catalog generated from 2-minute cadence TESS data during 2018 through 2022 (Sectors 1 to 54). This contains posterior estimates for 2,833 TESS Objects of Interest, including 151 multi-planet candidate systems and 68 candidates with data for only a single transit. Our analysis utilises the No-U-Turns Markov chain Monte Carlo algorithm to sample the parameter space with a circular transit model implemented in *exoplanet*. To enable follow-up as our understanding of the underlying populations evolves, we provide posterior samples from our analyses and Jupyter notebooks to reproduce the analyses for each exoplanet candidate.

Keywords: methods: data analysis — methods: statistical — miscellaneous — catalogs — surveys

1. INTRODUCTION

In July 2020, NASA’s Transiting Exoplanet Survey Satellite (Ricker et al. 2015) completed its two-year Primary Mission to search for transiting exoplanets around nearby bright stars. TESS recorded 2-minute cadence observations for $\sim 200,000$ pre-selected stars that were processed by the TESS Science Processing Operations Center (Jenkins et al. 2016) pipeline. Additionally, TESS also recorded measurements of its entire field of view in 10 and 30-minute sampled full-frame images (FFIs), enabling the flux measurements of tens of millions of stars. Between 2, 10 and 30-minute observations, the TESS Primary Mission and the ongoing extended missions have identified over 5,488 planet candidates, 227 of which have been confirmed as planets (Stassun et al. 2018, 2019; Guerrero et al. 2021; Guerrero & TESS Science Office 2021). Furthermore, TESS data have provided numerous non-exoplanet candidates disclosing new information on eclipsing binaries (e.g.,), and tidally interacting systems (e.g.,), exomoons (e.g.,), comets (e.g.,), exocomets (e.g.,), supernovae (e.g.,), and more (see [review] for more). *TODO: get citations.*

In this work we provide a comprehensive catalog of transiting exoplanet posterior estimates for the 2,833 TESS Objects of Interest (TOIs) with 2-minute cadence observations from 2018 through 2022. The posterior distributions provide robust uncertainties for the circular transit model’s planet orbital timing parameters, stellar limb darkening, stellar density, mean flux and detector noise parameters. The posterior distributions can allow future researchers to study the planet population in

detail and assess the reliability of the most Earth-like candidates, *TODO: list more things that can be done.*

The remainder of the paper is organised as follows: Section 2 describes our transit light curve model and the Bayesian framework we use to estimate parameters of exoplanet systems from the observed data. The analysis results are summarised in Section 3. The catalog, released data, and software to reproduce the results are described in Section 4 and are available online as supplementary materials (<http://catalog.tess-atlas.cloud.edu.au/>). Finally, we provide concluding remarks in Section 5.

2. METHOD

TODO: TOI selection, lightcurve preprocessing, eccentricity posterior postprocessing

2.1. Transit light curve model

There are many options for parameterisation of a transit, but we choose to model these transits as circular, non-interacting Keplerian orbits around their host star, parameterised by their observables. We approximate the host star’s stellar limb darkening profile using Kipping (2013)’s quadratic limb darkening law. Finally, we compute the exoplanet’s resultant quadratic limb-darkened transit lightcurve using an analytical model implemented in *starry*. The stellar variables in this model are parameterised by the baseline relative flux of the light curve f_0 , the mean stellar density ρ_* , and two parameters describing the quadratic limb-darkening profile of the star u_1, u_2 . To model stellar variability (e.g. asteroseismic oscillation of the star) we use a Gaussian Process implemented in *celerite* with a stochastically driven damped harmonic

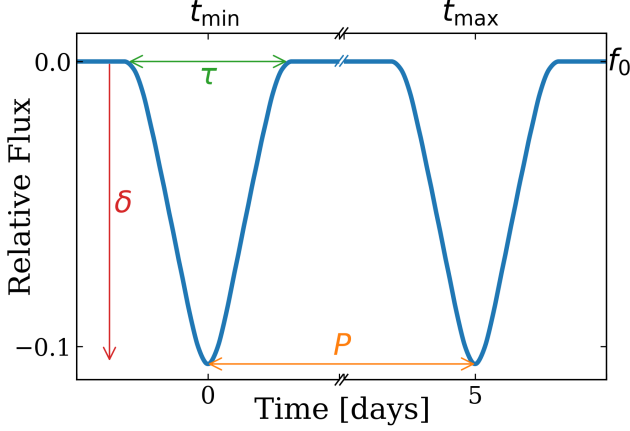


Figure 1. Schematic diagram of a transit light curve: *TODO: write some details about this plot*

oscillator kernel in linear combination with a jitter term, to capture misspecified error bars and model misspecification. This requires three parameters: the quality factor Q_{GP} , the undamped period of the oscillator ρ_{GP} , the standard deviation of the process σ_{GP} .

Each of the n exoplanets in the system are parameterised by the planets'

1. *two reference transit times*, one near the beginning of the observations, $t_{\min}[n]$, and one near the end, $t_{\max}[n]$, measured in TESS BJD,
2. *the approximate transit depth*, $\delta[n]$, measured in parts-per-thousand,
3. *the impact parameter* of the orbit, $b[n]$, constrained to be $|b| \leq 1$, and
4. *the transit duration*, $\tau[n]$, measured in hours,
5. *the radius ratio* $k[n]$ of the planet radius $R_p[n]$ divided by the stellar radius R_\star .

In the case when there are a planet has only a single transit present in the data, we use the planet's orbital period $P[n]$ in place of the second reference time $t_{\max}[n]$. We also track the relevant Jacobians of the parameters. Some of these parameters are displayed in the schematic diagram in Figure 1.

More discussion of the details, motivations, and limitations of this transit parameterisation are presented below.

Transit times—To speed up the analysis, we assume that the discovery period and phase of the orbit are close enough to the truth that we can fit only the data near the expected transit times. One consequence of this assumption is that we are assuming that the *number*

of periods that occur in the TESS observational baseline is correct. Practically, this means that our prior assumption is that the transits must occur within the data cutouts. This can be difficult to enforce—especially for low signal-to-noise transits—but a good approximation can be achieved by fitting for two reference transit times, t_{\min} and t_{\max} , with a fixed number of periods, N_P , between them, instead of a single reference time and the period. Then we can compute the implied period as $P = (t_{\max} - t_{\min})/N_P$. Importantly this does not change the prior on P and t_0 since the Jacobian is a constant $1/N_P$.

Transit depth—It is worth spending a moment on the transit depth parameterisation. This choice of parameterisation leads to efficient computation and convergence, but it comes with non-trivial shortcomings. Since the physical parameter that is required to compute the light curve model is the radius ratio between the planet and the star $k = R_p/R_\star$, we need to choose a parameterisation that is invertible and that isn't generally possible. In some cases, using radius ratio directly as the parameter can work well, but *TODO: explain cases where it's not*. Instead, we choose to parameterise the approximate transit depth δ using the small planet approximation. This is useful because it is directly invertible (conditioned on the limb darkening parameters and impact parameter), but it restricts us to considering non-grazing transits with impact parameter $|b| \leq 1$. Accepting this restriction, we can compute the approximate transit depth for a limb darkened light curve by assuming that the intensity of the star is uniform under the disk of the planet. For quadratic limb darkening, the intensity profile is

$$I(r) = 1 - u_1 [1 - \mu(r)] - u_2 [1 - \mu(r)]^2 \quad (1)$$

where $\mu(r) = \sqrt{1 - r^2}$. The ratio of the occulted flux to the total stellar flux when the transit is deepest ($r = b$) is (the same results are discussed by ??)

$$\delta \approx \frac{\int_0^k 2\pi r I(b) dr}{\int_0^1 2\pi r I(r) dr} = \frac{k^2 (1 - u_1 [1 - \mu(b)] - u_2 [1 - \mu(b)]^2)}{1 - u_1/3 - u_2/6} \quad (2)$$

Therefore, since k must be positive, we have a one-to-one transformation between δ and k conditioned on impact parameter $|b| \leq 1$ and the limb darkening coefficients. It is also important to include the Jacobian factor so that fitting in δ doesn't introduce a strange prior on r . In this case, the relevant factor is

$$\left| \frac{dk}{d\delta} \right| = \left| \frac{1 - u_1/3 - u_2/6}{2k (1 - u_1 [1 - \mu(b)] - u_2 [1 - \mu(b)]^2)} \right| \quad (3)$$

149 *Impact parameter*—Constrained to be non-grazing. –
 150 *TODO: Discuss the consequences of this.*

151 *Transit duration*—The physical parameter required for
 152 computing the transit model is the semi-major axis, a , in
 153 units of the stellar radius, but the transit duration τ is
 154 better constrained so it can be better as a fit parameter.
 155 For a circular orbit, the transit duration is (?)

$$156 \quad \tau = \frac{P}{\pi} \sin^{-1} \left(\frac{\sqrt{(1+k^2) - b^2}}{a \sin i} \right) \quad . \quad (4)$$

157 Rearranging this, we find

$$158 \quad a^2 \sin^2 i \sin^2 \left(\frac{\pi \tau}{P} \right) = (1+k^2) - b^2 \quad . \quad (5)$$

159 Then, using the fact that $\cos^2 i = b^2/a^2$, we find

$$160 \quad a^2 = \frac{(1+k)^2 - b^2 \cos^2 \phi}{\sin^2 \phi} \quad (6)$$

161 for $\phi = \pi \tau/P$. And the Jacobian is

$$162 \quad \frac{da}{d\tau} = \frac{\pi \cos \phi}{a P \sin^3 \phi} [b^2 - (1+k)^2] \quad . \quad (7)$$

163 Finally, from the period and semi-major axis, we can
 164 compute the implied stellar density (under this assump-
 165 tion of a circular orbit)

$$166 \quad \rho_{\text{circ}} = \frac{3 \pi a^3}{G P^2} \quad . \quad (8)$$

167 It is important to note that this is not necessarily the
 168 same as the actual stellar density and that, in a multi-
 169 planet system, this implied density won't be the same
 170 for each planet (see, for example, ??).

171 2.2. Bayesian Framework

172 Likelihood, GP, Priors, celerite, pymc3 sampling

173 3. RESULTS

174 3.1. Systems with multiple planets

175 Some words about these systems

176 3.2. Planets with data for one transit

177 Some stuff about single transit systems

178 4. DATA AND SOFTWARE AVAILABILITY

179 We provide software to reproduce the analyses and
 180 results at <http://catalog.tess-atlas.cloud.edu.au/>. The

181 website contains one Jupyter notebook for each TOI,
 182 demonstrating the end-to-end analysis of a TOI. The
 183 notebooks contain software to download and clean light
 184 curve data, implementations of the transit-model and
 185 priors for inference, the PyMC3 sampling stage, and a
 186 posterior post-processing step. The website also docu-
 187 ments the method to download our Bayesian parameter
 188 inference posterior samples, load them and make various
 189 plots.

190 5. DISCUSSION

191 We present for the first time a catalog of Bayesian
 192 posterior samples for the 2-minute cadence TOIs from
 193 2018-2022. Some words about results. Some stuff about
 194 difficulty sampling grazing systems. Errors when SPOC
 195 estimates are off. We expect the remainder of the TESS
 196 extended mission will complete by September 2023, at
 197 which point an updated catalog will be produced.

198 We would like to thank xyz. Ozgrav, Flatiron, NEC-
 199 TAR, ADACS, David Liptai Work was started during
 200 'online.tess.science'

201 This work has made use of the TIC through the TESS
 202 Science Office's target selection working group (archi-
 203 tects K. Stassun, J. Pepper, N. De Lee, M. Paegert, R.
 204 Oelkers).

205 This research has made use of the NASA Exoplanet
 206 Archive, which is operated by the California Institute
 207 of Technology, under contract with the National Aero-
 208 nautics and Space Administration under the Exoplanet
 209 Exploration Program.

210 This work made use of the TESS catalog on ExoFOP
 211 Total compute time for this work $\sim 80,000$ Hrs *TODO:*
 212 *get more accurate compute time (this is an overestimate).*
 213 CO₂ emission amount for this work would be XX, how-
 214 ever as OzStar uses wind energy this has a negligible
 215 carbon footprint.

216 *Facilities:* TESS, Gaia, Kepler, Exoplanet Archive,
 217 etc.

218 *Software:* astropy (??), exoplanet, lightkurve, starry,
 219 celerite2, pymc3, numpy, scipy, pandas, matplotlib, cor-
 220 ner, sphinx,

REFERENCES

- 221 Guerrero, N., & TESS Science Office. 2021, in American
 222 Astronomical Society Meeting Abstracts, Vol. 53,
 223 American Astronomical Society Meeting Abstracts, 117.01
- 224 Guerrero, N. M., Seager, S., Huang, C. X., Vanderburg, A.,
 225 & et al. 2021, ApJS, 254, 39,
 226 doi: [10.3847/1538-4365/abef1](https://doi.org/10.3847/1538-4365/abef1)

- 227 Jenkins, J. M., Twicken, J. D., McCauliff, S., Campbell, J.,
228 & et al. 2016, in Society of Photo-Optical Instrumentation
229 Engineers (SPIE) Conference Series, Vol. 9913, Software
230 and Cyberinfrastructure for Astronomy IV, ed. G. Chiozzi
231 & J. C. Guzman, 99133E, doi: [10.1117/12.2233418](https://doi.org/10.1117/12.2233418)
- 232 Kipping, D. M. 2013, MNRAS, 435, 2152,
233 doi: [10.1093/mnras/stt1435](https://doi.org/10.1093/mnras/stt1435)
- 234 Ricker, G. R., Winn, J. N., Vanderspek, R., Latham, D. W.,
235 & et al. 2015, Journal of Astronomical Telescopes,
236 Instruments, and Systems, 1, 014003,
237 doi: [10.1117/1.JATIS.1.1.014003](https://doi.org/10.1117/1.JATIS.1.1.014003)
- 238 Stassun, K. G., Oelkers, R. J., Paegert, M., Torres, G., &
239 et al. 2019, AJ, 158, 138, doi: [10.3847/1538-3881/ab3467](https://doi.org/10.3847/1538-3881/ab3467)
- 240 Stassun, K. G., Oelkers, R. J., Pepper, J., Paegert, M., &
241 et al. 2018, AJ, 156, 102, doi: [10.3847/1538-3881/aad050](https://doi.org/10.3847/1538-3881/aad050)